Vol 13 No 2, February 2004
1009-1963/2004/13(02)/0190-06
Chinese Physics
© 2004 Chin. Phys. Soc.
and IOP Publishing Ltd

Basic characteristics of an atmospheric pressure rf generated plasma jet

Wang Shou-Guo(王守国)†, Li Hai-Jiang(李海江),
Ye Tian-Chun(叶甜春), and Zhao Ling-Li(赵玲利)

Microelectronics Research and Development Center, Chinese Academy of Sciences, Beijing 100010, *China*

(Received 20 May 2003; revised manuscript received 10 October 2003)

A plasma jet has been developed which operates using radio frequency (rf) power and produces a stable homogeneous discharge at atmospheric pressure. Its discharge characteristics, especially the dependence of stable discharge operating range on the feed gas, were studied, and the electric parameters such as RMS current, RMS voltage and reflected power were obtained with different gas flows. These studies indicate that there is an optimum range of operation of the plasma jet for a filling with a gas mixture of He and O_2. Two "failure" modes of the discharge are identified. One is a filamentary arc when the input power is raised above a critical level, another is that the discharge disappears gradually as the addition of O_2 approaches 3.2%. Possible explanations for the two failure modes have been given. The current and voltage waveform measurements show that there is a clear phase shift between normal and failure modes. In addition, I–V curves as a function of pure helium and for 1% addition of oxygen have been studied.

Keywords: atmospheric pressure, plasma jet, discharge model
PACC: 5250D, 5280P

1. Introduction

Recently, much attention has been paid to gas discharges for producing atmospheric pressure nonthermal plasma, and a few novel atmospheric pressure discharge sources have been developed. These sources include the atmospheric pressure plasma jet (APPJ),[1−7] the dielectric barrier (silent) discharges (DBD),[8,9] the one atmosphere uniform glow discharge plasma (OAUGDP),[10] and the surface-wave discharge.[11] They show promise to potentially replace low-pressure plasma devices for some existing applications such as sterilization, disinfecting, cleaning, decontamination, surface treatment, food processing, etching, thin film deposition and so on. In principle, however, atmospheric pressure plasma can provide a critical advantage over the widely used low-pressure plasma, for they do not require expensive and complicated vacuum systems. Without a vacuum system, not only the cost of materials processing could be reduced substantially, but also the operating constraints due to a chamber-based process will disappear.

Among all of these sources, the APPJ is a unique, nonthermal, glow-discharge plasma operating at atmospheric pressure. The discharge uses a high-flow feed gas consisting primarily of helium as a carrier gas and a small amount of reactive gases (e.g., O_2, H_2O or CF_4) in a capacitively coupled configuration using radio frequency (rf) power which causes the gas breakdown and produces a stable oscillating steady-state discharge in a coaxial arrangement without dielectric materials between the electrodes. The feed gas becomes excited, dissociated or ionized by energetic electron impact. Once it exits the discharge volume, ions and electrons are rapidly lost by recombination, leaving behind metastable species (e.g., O^*, He^*) and radicals (e.g., O, OH, F). These reactive species are then directed onto a surface where the desired chemical reaction occurs. In this way, the surface to be treated does not require immersion in the source and is not directly exposed to the plasma. Furthermore, due to the low temperature of the effluent (clearly below 100°C) no thermal problems evolve even on sensitive materials. So far, the APPJ has been used to etch polyimide, tungsten, tantalum, and silicon dioxide; to deposit silicon dioxide and silicon nitride films;[7,12,13] and to decontaminate chemical and biological warfare agents.[14]

Compared with low-pressure plasma devices, the

†E-mail: sgwang3@yahoo.com.cn

APPJ has obviously a lot of advantages, such as no need for expensive vacuum equipment and no constraint to a chamber-based process, but there still exist drawbacks during the practical applications, such as using a large amount of relatively expensive helium as carrier gas and small amount of oxygen. Therefore, it is very necessary to study the corresponding discharge operating range and physics on the feed gas to find the optimum way to reduce the feed gas cost during the practical use of the APPJ. On the other hand, much of the effort in generating stable glow discharges at atmospheric pressure has focused on preventing the onset of instabilities, particularly in the glow-to-arc transition. It is especially important to understand the mechanism of how the arcing happens.

In this report, we introduce the device recently developed in our group and present its basic operation, in particular the effect of mixing helium with oxygen on the discharge process of the APPJ, because the mixture of helium and oxygen is a typical feed gas for practical applications. These studies indicate that the operation of the plasma jet shows an optimum range in the gas parameters (e.g., composition, flow). The dependence of the gas flow on discharge operating conditions has been determined. The current and voltage waveform measurements show that there are two failure modes: one is the "conventional arcing" mode which we call "phase-shift-backward", and the other is the "gradual disappearance" mode which we call "phase-shift-forward". These two modes are useful for understanding how the APPJ fails during the operations and will be helpful to prevent the failure.

2. Experimental setup

A schematic of the experimental setup is shown in Fig.1. A gas mixture of helium and oxygen was fed through an annular region between the two stainless steel coaxial electrodes 10 cm in length without the nozzle. The inner electrode was 12 mm in diameter and was connected to a rf generator operating at typically 13.56 MHz, while the outer electrode was separated from the inner electrode by a gap 1.25 mm and was grounded. Two electrodes that operate in a capacitively coupled configuration were cooled with water. The feed gases, helium and oxygen, were mixed using a gas mixing system (WITT-Gasmischer, KM100-2), and then passed through the annular space between the electrodes.

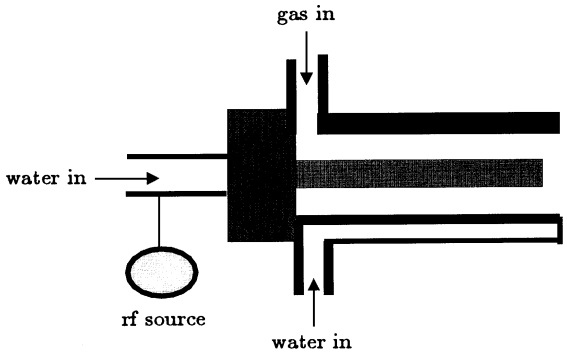


Fig.1. Schematic of the plasma jet.

The electrical properties of the discharge were studied simultaneously by measuring the voltage across the discharge and rf current. The measurements were made using a high voltage probe (Tektronix P6015A with a bandwidth of 75 MHz) and a current probe (Tektronix P6021, with a bandwidth of 60 MHz). The results were recorded on a digital oscilloscope (Tektronix TDS 210 with sampling rate of a 1 G samples/s and a bandwidth of 60 MHz) with triggering on the voltage signal. Measurements were conducted for different gas flow rates and different oxygen contents.

3. Experimental results

Based on the various operation conditions, such as gas flow, input power, electrode constructions, gap spacing, once the design of the APPJ has been finished, its geometry usually cannot be changed easily during the discharge process, and what we can do is to adjust the input power and gas compositions. After a discharge in the APPJ is initiated by using pure helium when the breakdown voltage is reached, the plasma emission intensity, the discharge voltage and rf current increase monotonically with increasing input power. Subsequently, i.e. after having reached a stable operation, the feed gas will usually be modified. Visual inspection of the discharge between the electrodes reveals a uniform glow with an apparent arcing, while there is virtually a weak emission outside the discharge region about 10 mm in length due to very rapid electron cooling. Figure 2(a) shows the dependence of the reflected power on the pure helium with the addition of 1% oxygen. The reflected power varies with the different amount of total gas flow when the forward power of the rf power source is kept constant. The results show that there is a relative optimum operation range of the total gas flow from 1.5 to 3.5 m^3/h; in this region the reflected power is a

minimum.

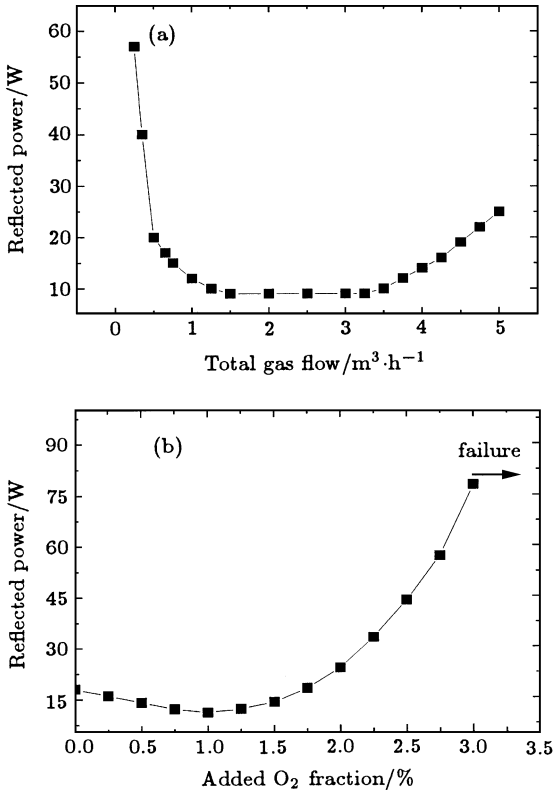


Fig.2. The dependence of the reflected power on: total flow of He+1% O_2 (a); the addition of O_2 (b). Other discharge parameters: gap spacing is 1.25 mm, rf frequency is 13.56 MHz, forward power is 260 W, and at 1.01×10^5 Pa.

With changing the content of oxygen, the reflected power versus the content of oxygen is shown in Fig.2(b), while the total gas flow rate is kept 1.5 m^3/h. When the content of oxygen is less than 1%, the reflected power decreases slightly with increasing oxygen content, and the minimum reflected power is found at about 1% oxygen. However, the reflected power will increase rapidly with further increase of oxygen content; actually, the reflected power becomes very sensitive to the content of oxygen when it approaches 3%, and the discharge also becomes unstable. In addition, the corresponding RMS current and voltage have been studied, as shown in Figs.3 and 4. Comparing Figs.3(a) and (b), we can identify that the RMS current and voltage vary oppositely with increasing total gas flow, a larger change is found as the total flow rate changes from 0.5 to 1 m^3/h, and the largest RMS current and the least RMS voltage have been found at the gas flow rate about 2 m^3/h, at which the optimum reflected power has already been attained, as shown in Fig.3(a). Another oppositely varying phenomenon between the RMS current and voltage is shown in Figs.4(a) and (b) with increasing content of oxygen. Figure 4(a) shows that the RMS voltage increases monotonically, and Fig.4(b) shows that the RMS current decreases monotonically. Comparing the changes of current and voltage, the RMS current is more sensitive to gas flow and oxygen content than the RMS voltage.

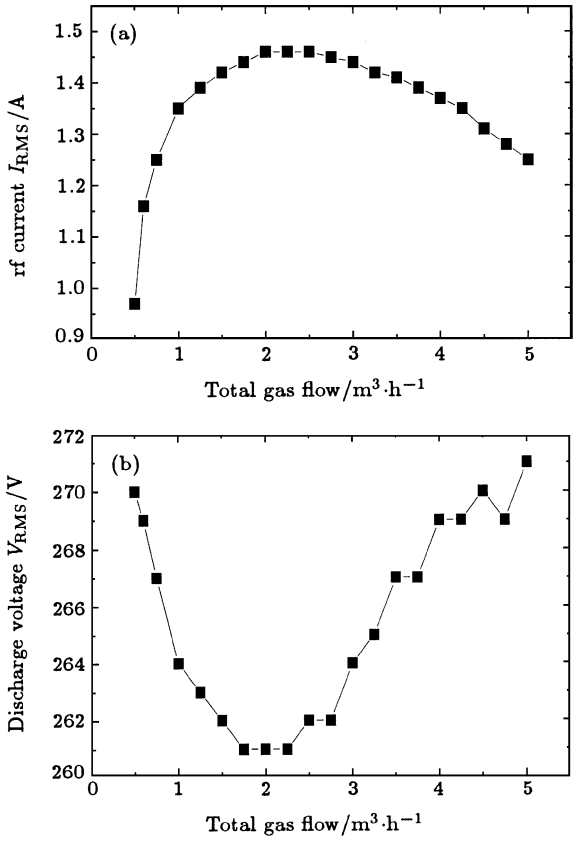


Fig.3. The rf current (a) and discharge voltage (b) as functions of total gas flow. Other discharge parameters: gap spacing is 1.25 mm, rf frequency is 13.56 MHz, forward power is 260 W, and at 1.01×10^5 Pa.

Figure 5 shows the waveforms of discharge voltage and rf current for normal discharge (solid line) and the arcing (dotted line). At low powers, the voltage and current waveforms are nearly sinusoidal, and a 78° phase difference between them means that the load is mostly capacitive. Both the current and the discharge voltage increase linearly with increasing input power. When the input power is raised above a critical level (230 W), the discharge suddenly turns into a filamentary arc; in the meanwhile, the input power goes down to 165 W, causing a highly localized and bright orange emission, and a clear "phase-shift-backward" of current waveform appears between the normal discharge and the arcing. The amplitude of the rf current reduces a little; however, the discharge voltage decays substantially, which results in the reduction of input

power to about 80% of the primary value. It is noted that usually the arcing spots are found near the end of electrodes in our system.

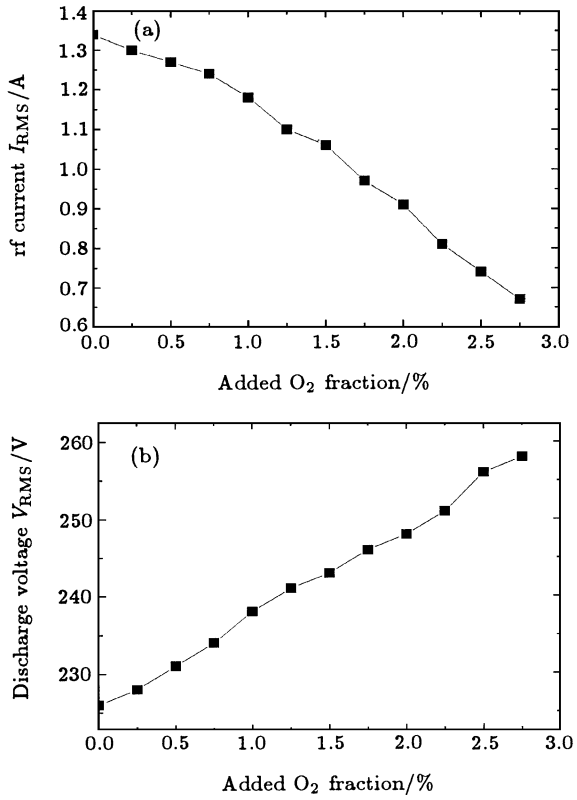


Fig.4. The rf current curve (a) and discharge voltage curve (b) as a function of the oxygen content in pure helium. Discharge parameters: total gas flow rate is 2 m^3/h, gap spacing is 1.25 mm, forward power is 260 W, and rf frequency is 13.56 MHz.

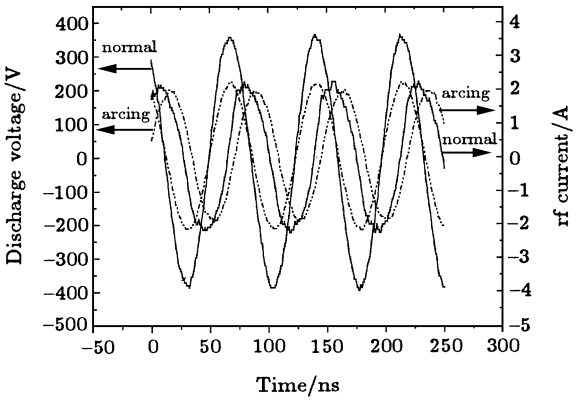


Fig.5. Waveforms of the discharge voltage and the rf current for the normal (solid line) and arcing (dotted line) modes in a pure helium discharge. Discharge parameters: He flow rate is 2 m^3/h, gap spacing is 1.25 mm, input power is 230 W directly before arcing, input power for arcing mode is 165 W.

In comparison, Fig.6 shows waveforms of the discharge voltage and rf current which present another failure mode. When the addition of oxygen varies as 1%, 2.8%, 3%, and 3.2%, the corresponding waveforms of the discharge voltage and rf current are V_1 and I_1, V_2 and I_2, V_3 and I_3, V_4 and I_4, respectively. With the increase of the oxygen content, the amplitude of the discharge voltage changes slightly; however, the amplitude of the rf current decreases dramatically, particularly when the addition of oxygen is up to 3.2%—the amplitude of the rf current drops rapidly to the original value before the gas is ignited; in the meantime, its phase difference vanishes rapidly so as to be in phase with the voltage waveform, indicating that the load becomes an infinite resistance and the discharge disappears entirely. However, it seems that there is still a little current as shown by the curve I_4; perhaps it belongs to a disturbance caused by the rf power source. We call this kind of failure as "phase-shift-forward". This phenomenon indicates that as the load transfers from capacitance to infinite resistance, the feed gas under this condition cannot be ignited any more.

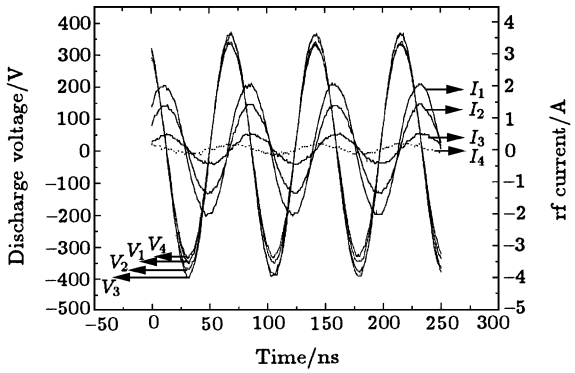


Fig.6. Waveforms of the discharge voltage and the rf current for different content (V_1 and I_1 for 1%, V_2 and I_2 for 2.8%, V_3 and I_3 for 3%, V_4 and I_4 for 3.2%) of oxygen in pure helium. Other discharge parameters: total gas flow rate is 2 m^3/h, gap spacing is 1.25 mm, input power is 250 W.

Now we discuss some power dependences. Figure 7 shows I–V curves which are very similar to the data for the plane-parallel setup of the APPJ described in Ref.[6]. In our case, the arcing appears suddenly for the pure helium discharge when the input power is raised to 230 W, as shown in Fig.7 (a). At this moment, the values of rf current and discharge voltage go down from A to B. Reducing the input power, the I–V curve goes from B to C, representing the "phase-shift-forward" mode, while the arcing coexists with a uniform glow. Further reducing the input power to about 100 W, the discharge returns to the path prior to arcing from C to D. When we use the pure helium

mixed with 1% oxygen, no arcing has been found when the rf power source changes from 1 to 300 W, which we use in this work, as shown in Fig.7(b); about this result we do not have a final understanding so far. Probably, it depends on the lower degree of ionization within the oxygen containing discharge and the connected different EEDF that will probably contain less energetic electrons. This will result in a lower, which in our case is desired, chance to ignite an arc.

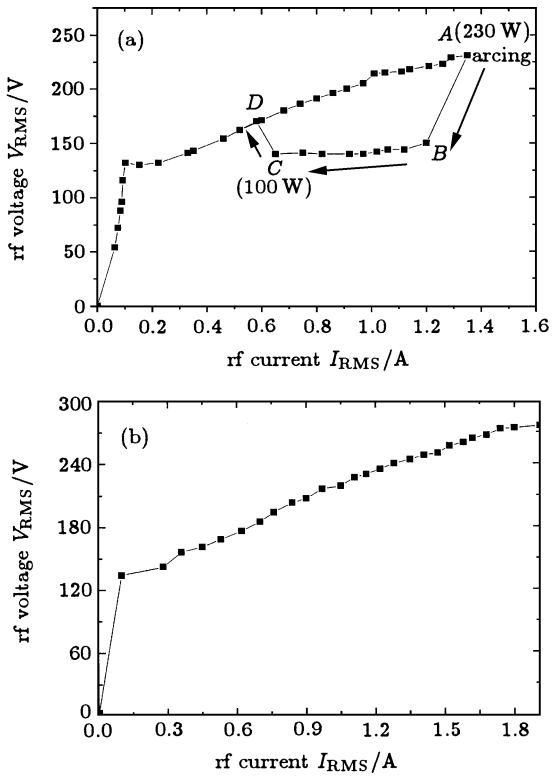


Fig.7. *I–V* curves as a function of rf current for pure helium discharge (a) and for 1% oxygen in pure helium (b). Discharge parameters: gas flow rate is 2 m^3/h, gap spacing is 1.25 mm, and rf frequency is 13.56 MHz.

4. Discussion

For practical use, an optimum range of operation of the APPJ has been found as it is filled with an helium and oxygen mixture at a rate from 1.5 to 3.5 m^3/h, at which the discharge is stable with a minimum reflected power. Furthermore, Fig.4 indicates that the RMS current is the largest when the feed gas is about 2 m^3/h, which means that it will be the optimum gas flow rate for obtaining the best ionized feed gas, so that in practical application it is actually not necessary to use more gas flow than that needed, considering the cost of the gas supply. For the mixing of oxygen, Figs.2–4 indicate that the optimum content of oxygen is 1%–2%. These results indicate that the discharge properties at atmospheric pressure are more sensitive to gas composition than to the total gas flow, and that the corresponding rf currents are more sensitive than the corresponding discharge voltages. It has been noted that the discharge parameters vary a little for day by day measurements, possibly due to the changes in the surface condition of the electrodes.

Regarding the arcing failure mode, as shown in Figs.5 and 7(a), it is probably a phenomenon of electrons avalanche caused by fast electrons, which will easily happen at high pressures. To prevent this, it is necessary to reduce the rf current, especially the fast electrons by adding a small amount of reactive gas, modifying the electrodes, and so on.

A new "failure" mode has been first identified in our system when the addition of oxygen is over 3%, as shown in Fig.6. With this failure mode, no filamentary arc has been found, but the amplitude of the rf current reduces gradually to zero, and the reflected power increases substantially, as shown in Fig.2(b), until it nearly equals the forward power while the discharge has already disappeared. Another apparent feature in this mode is that the phase of rf current waveform goes forward by about 78°, while in the conventional arcing mode in Fig.5 the current phase-shift goes forward about 30° as the voltage signal is triggered.

One possible explanation for this failure mode is that the capacitance between the two electrodes changes too much when the addition of oxygen is up to 3.2% so that the power cannot be coupled into the feed gas, which results in a failure of the discharge. As compared with the low-pressure plasma, the feature of atmospheric pressure plasma is the presence of finite and relatively large electric fields in the bulk region to drive the electron conduction current because of the low mobility of electrons, as shown as follows:

$$I_{\rm rf} \approx I^{\rm e}_{\rm cond} = -n_{\rm e} e \mu_{\rm e} A E_{\rm bulk}$$

and

$$A = \pi(D_2 + D_1)L,$$

where $I_{\rm rf}$ and $I^{\rm e}_{\rm cond}$ are the rf current and the electron conduction current in the bulk, $n_{\rm e}$ is the electron density, $\mu_{\rm e}$ is the electron mobility, A is the cross sectional area in the middle of the gap spacing, $E_{\rm bulk}$ is the mean electric field in the bulk region, D_2 and D_1 are respectively the inner diameter of the grounded electrode and the outer diameter of the rf electrode, and L is the length of the electrodes. It is assumed

that the displacement current is small compared with the electron conduction current in the bulk region.

With the simple relation among the rf current, the capacitance and the discharge voltage, as shown in

$$I_{\mathrm{rf}} = (\mathrm{i}\omega C_{\mathrm{sheath}})V_{\mathrm{sheath}},$$

where ω is the angular frequency of the rf fields, C_{sheath} is the sheath capacitance, V_{sheath} is the voltage across the sheath, we can easily derive the following equation:

$$C_{\mathrm{sheath}} = \mathrm{i}n_{\mathrm{e}}e\mu_{\mathrm{e}}AE_{\mathrm{bulk}}/\omega V_{\mathrm{sheath}}.$$

It can be identified that the sheath capacitance strongly depends on the electron density. Considering that the oxygen molecule has more and higher energy levels than the helium atom, when oxygen is added to a critical level, more and higher energy levels per unit-volume will absorb a large number of conduction electrons, which results in a significant decrease of electron density, and finally leads to the disappearance of discharge. On the other hand, the two sheath capacitances also vary so much at the same time with the change of electron density, that the forward power cannot be coupled into the feed gas. However, further study and understanding of the nature of this "failure" mode at this point is needed.

The "phase-shift-forward" mode was not found during the increase of gas flow. This is because the pressures on both sides of the plasma jet change only slightly during the increase of the gas flow. The main change is the flow velocity of the plasma jet, hence the density of the feed gas per unit-volume between the electrodes does not change too much. These results further indicate that the discharge properties of the plasma jet at atmospheric pressure are more sensitive to the gas composition than to the total gas flow.

5. Conclusions

Some fundamental issues which are important for the practical application of helium with the addition of oxygen are presented in the APPJ that we recently developed. An optimum range of operation of the plasma jet as it was filled with helium and oxygen mixture has been defined from 1.5 to 3.5 m^3/h and the addition of oxygen is from 1% to 2%, The best ionized feed gas will be obtained when the total gas flow is equal to 2 m^3/h, also this may not be the mode of operation where the optimum dissociation is reached.

Two "failure" modes of the discharge have been identified. The current and voltage waveform measurements show that there are clear phase shifts between normal and failure modes, which will be useful to control the operation automatically. A new failure mode called "phase-shift-forward" has been first identified in our system when the addition of oxygen is above the critical level, in which the discharge disappears gradually.

References

[1] Babayan S E, Joeng J Y, Tu V J, Park J, Selwyn G S and Hicks R F 1998 *IEEE Trans. Plasma Sci.* **26** 286

[2] Wang S G, Gathen V S and Doebele H F 2003 *Appl. Phys. Lett.* **83** 3272

[3] Tu V J, Jeong Y J, Schutze A, Babayan S E, Ding G, Selwyn G S and Hicks R F 2000 *J. Vac. Sci. Technol.* A **18** 2799

[4] Park J, Henins I, Herrmann H W and Selwyn G S 2001 *J. Appl. Phys.* **89** 15

[5] Selwyn G S, Herrmann H W , Park J and Henins I 2001 *Contrib. Plasma Phys.* **6** 610

[6] Park J, Henins I, Herrmann H W and Selwyn G S 2001 *J. Appl. Phys.* **89** 20

[7] Babayan S E, Joeng J Y , Tu V J, Park J , Selwyn G S and Hicks R F 1998 *Plasma Sources Sci. Technol.* **7** 286

[8] Eliasson B and Kogelschatz U 1988 *Appl. Phys.* B **46** 299

[9] Massines F, Rabehi A, Decomps P, Gadri R B, Segur P and Mayoux C 1998 *J. Appl. Phys.* **83** 2950

[10] Roth J R, Tsai P P Y, Liu C, Laroussi M and Spence P D 1995 *U. S. Patent,* No.5414324 Issued May

[11] Moison M, Zakrzewski Z, Etemadi R and Rostaing J C 1998 *J. Appl. Phys.* **83** 5691

[12] Babayan S E, Jeong J Y, Schütze A, Tu V J, Moravej M, Selwyn G S and Hicks R F 2002 *Plasma Sources Sci. Technol.* **10** 573

[13] Nowling G R, Babayan S E, Jankovic V and Hicks R F 2002 *Plasma Sources Sci. Technol.* **11** 97

[14] Herrman H W, Henins I, Park J and Selwyn G S 1999 *Phys. Plasma* **6** 2284